SUPPLEMENTARY INFORMATION

Functional Assembly of Nitrous Oxide Reductase provides Insights into Copper Site Maturation

Lin Zhang, Anja Wüst, Benedikt Prasser, Christoph Müller, and Oliver Einsle

Supplementary Figures

Supplementary Tables

Supplementary References

www.pnas.org/cgi/doi/10.1073/pnas.1903819116

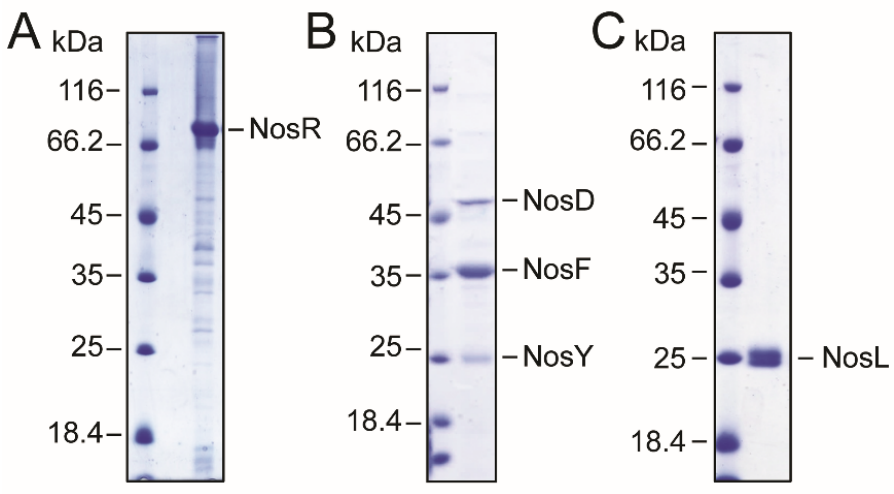

Figure S1. SDS-PAGE analysis of **A**) recombinant *Ps*NosR, **B**) *Ps*NosDFY and **C**) ***Ps*NosL**. *Ps*NosR and *Ps*NosF were His-tagged at either C-terminus or N-terminus; *Ps*NosL was Strep-tagged at the C-terminus. The molecular mass of *Ps*NosR, *Ps*NosD, *Ps*NosF, *Ps*NosY and *Ps*NosL are 81.9 kDa, 48.2 kDa, 33.8 kDa, 29.4 kDa and 20.4 kDa, respectively. The identity of the individual subunits was confirmed by mass-spectrometric analysis.

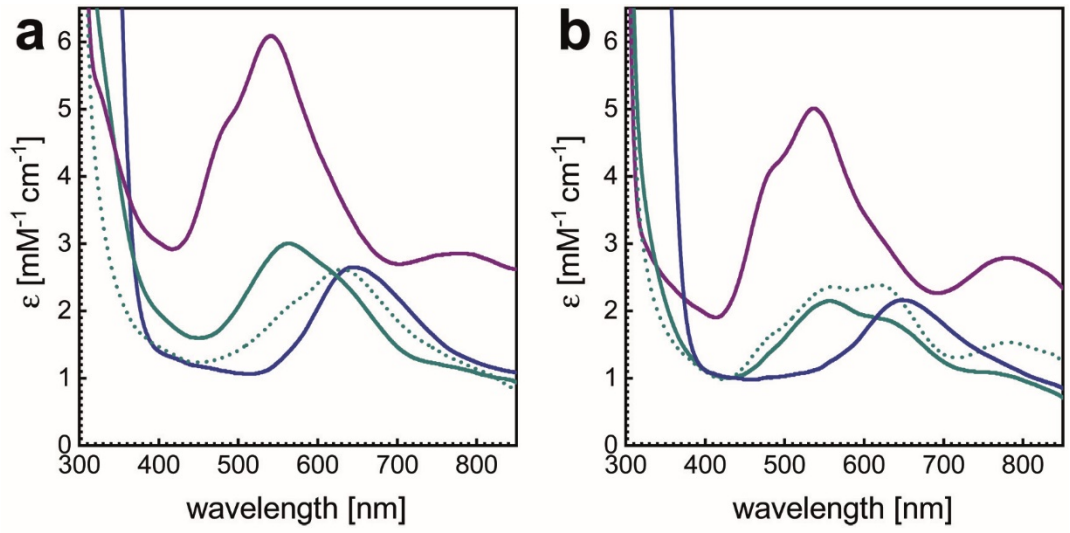

Figure S2: Electron excitation spectra of anoxically *vs*. oxically isolated rN_2OR. **A**) anoxic isolation, **B**) oxic isolation protocol. The spectrum of the protein as isolated is shown in cyan (dotted) in both panels. Samples were oxidized with potassium ferricyanide (purple) to yield form I spectra with maxima at 538 nm and 795 nm. Addition of ascorbate led to selective reduction of Cu_A (cyan), and further reduction by sodium dithionite yielded a blue form with a single charge-transfer band at 650 nm (blue). Beside a slightly elevated copper content in the anoxic preparation (A), both samples show nearly identical spectroscopic properties.

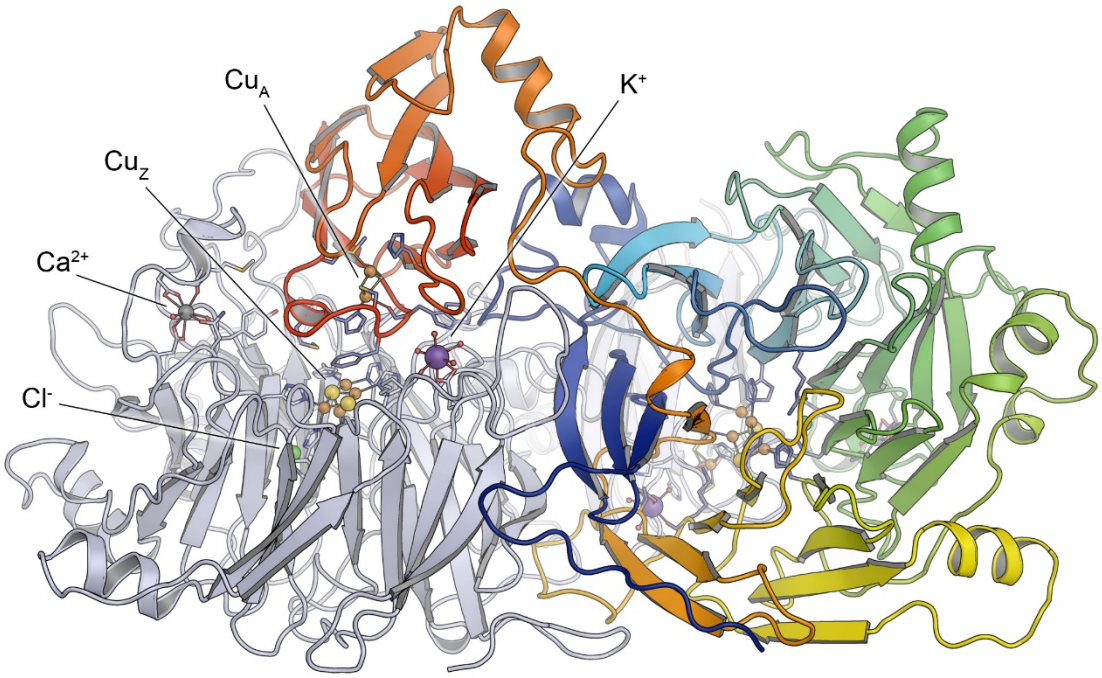

Figure S3: Three-dimensional structure of recombinant *Ps*NosZ. With an overall root-mean-squared displacement of 0.2 Å, the dimeric structure of recombinant *Ps*NosZ produced in *E. coli* is nearly identical to that of native protein isolated from *P. stutzeri* (PDB 3SBQ). The two peptide chains form a tight head-to-tail dimer that results in a close distance of 10 Å between the Cu_A and Cu_Z centers of different monomers. Monomer A is shown in grey cartoon, monomer B is colored from blue at the N-terminus to red at the C-terminus. The copper centers and metal ions are depicted as spheres, as are the calcium (gray), potassium (purple) and chloride ions (green) coordinated within each monomer.

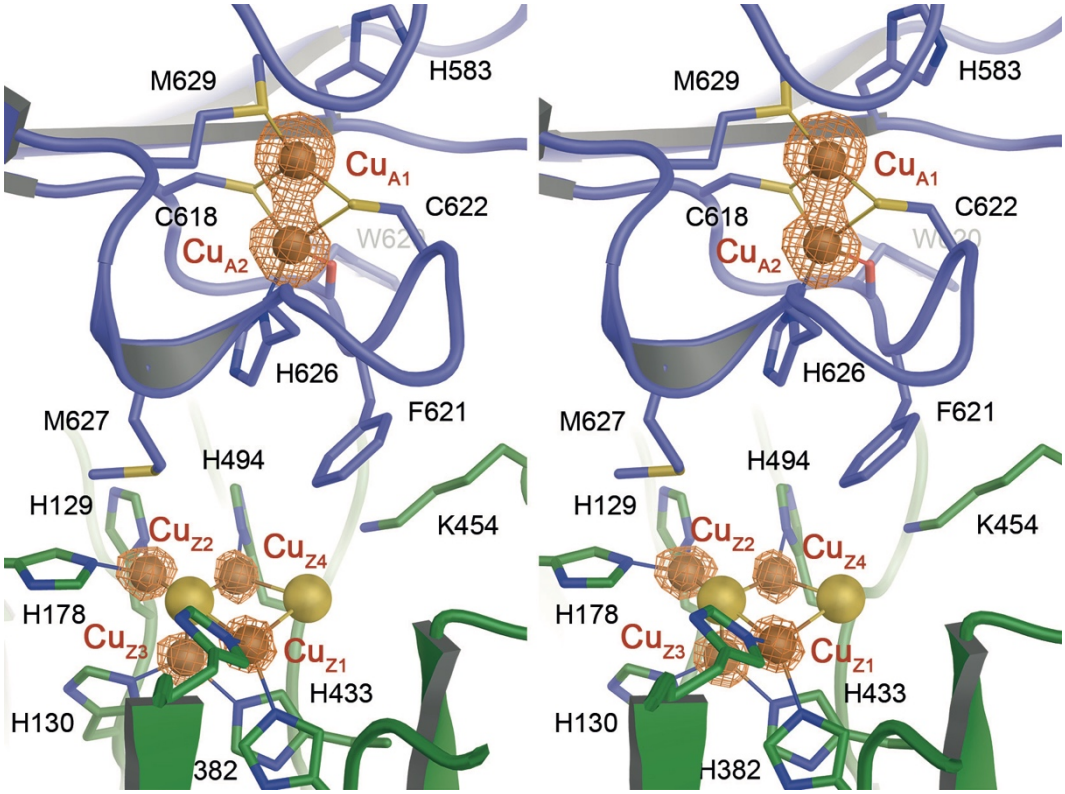

Figure S4: Anomalous difference Fourier electron density maps. The stereo image, analogous to Fig. 3e, shows an electron density map with anomalous differences as Fourier coefficients contoured at the 3.5 σ level. Residue H583 was found not to coordinate Cu_{A1} in any of the four monomers in the asymmetric unit. The contour map clearly indicates that while the metal sites in Cu_A were fully occupied, the Cu_Z centers showed a partial occupancy of approximately $q = 0.5$.

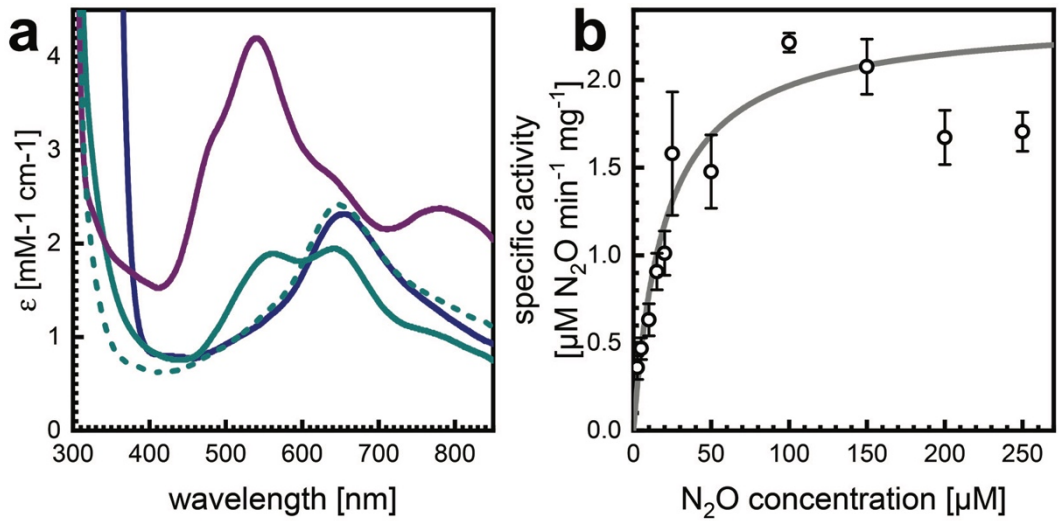

Figure S5: The role of NosR and ApbE in the maturation of *Ps*NosZ. rNosZ was produced without co-expression of *Ps*NosR and *Ps*ApbE (II in Table 1). **A**) Electron excitation spectra of rN_2OR. The protein was isolated in the blue form, with a single maximum at 650 nm (dashed). Oxidation with potassium ferricyanide turned the sample purple, yielding a form I spectrum with maxima at 538 nm and 780 nm (purple). Selective reduction of Cu_A by sodium ascorbate resulted in maxima at 562 nm and 640 nm (cyan), and further reduction by sodium dithionite re-formed the single peak at 650 nm (blue). **C**) Specific activity of rN_2OR (II) towards N_2O using reduced benzyl viologen as an electron donor. V_{max} and K_M were determined to 2.08 ± 0.10 µM N_2O min^{-1} mg^{-1} and 16.18 ± 3.01 µM, respectively, using a hyperbolic fit function according to the Michaelis-Menten equation.

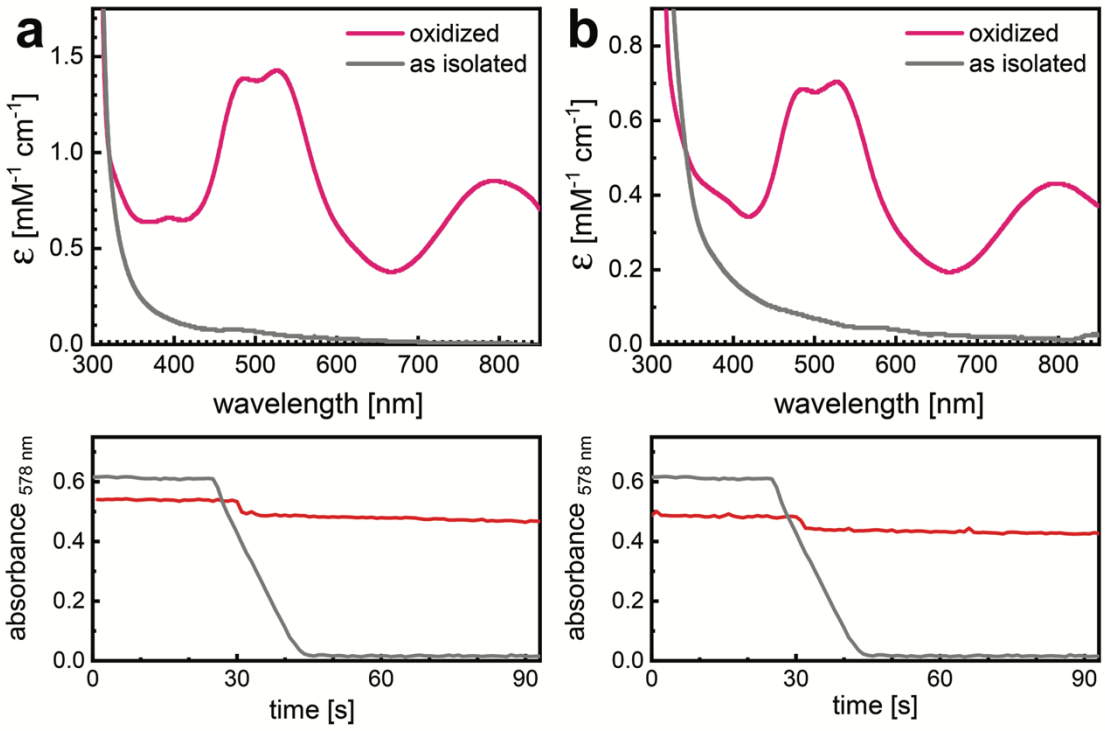

Figure S6: The role of NosDFY in the assembly of Cu_Z. **A**) rN_2OR could be produced without the co-expression of *Ps*NosRDFY and *Ps*ApbE (III in Table 1). As shown by electron excitation spectroscopy (above), the protein was colorless as isolated (grey). It turned pink upon oxidation by potassium ferricyanide, showing the spectral features of Cu_A, with maxima at 485 nm, 525 nm and 795 nm (pink). An activity assay (below) for *Ps*NosZ (III) using reduced benzyl viologen as electron donor and N_2O as a substrate showed no activity (pink). The grey curve represents a positive control using sample *Ps*NosZ (II). **B**) If rN_2OR was instead produced under co-expression of inactive *Ps*NosDFY ($E154Q^F$, IV in Table 1), the sample again only showed the spectral features of the Cu_A site (above, pink), albeit with a reduced occupancy, but not of Cu_Z. The corresponding activity assay for *Ps*NosZ (IV) on N_2O (below) again showed no activity of the sample (pink). The grey curve is the same positive control as in (A).

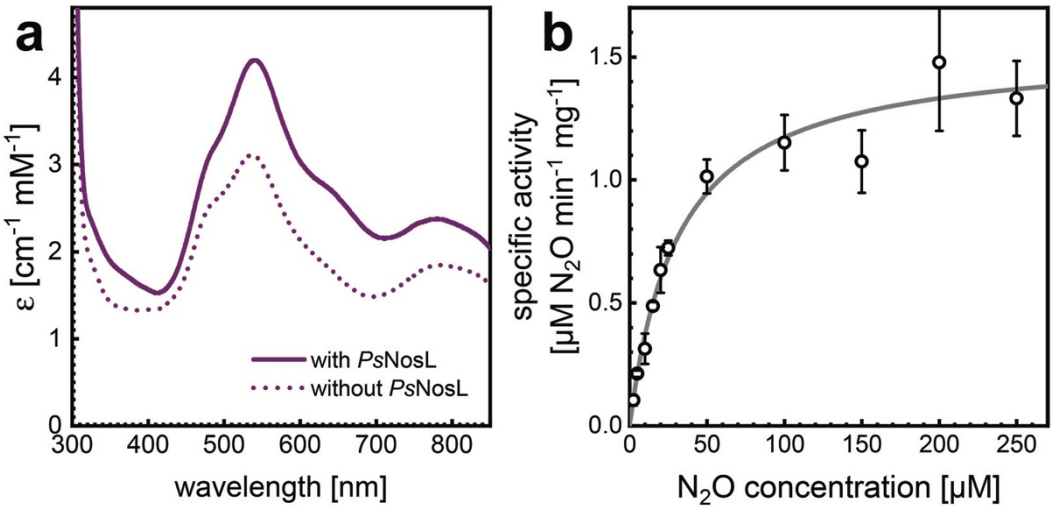

Figure S7: Role of *Ps*NosL in the copper site assembly of *Ps*NosZ. rN_2OR was produced with and without co-expression of *Ps*NosRL and *Ps*ApbE (V in Table 1). **A**) *Ps*NosZ (V) was isolated in the blue form (data not shown) and yielded a purple form I spectrum upon oxidation with potassium ferricyanide, with maxima at 538 nm and 785 nm (dotted). While the copper content was reduced in this preparation, the maturation of Cu_Z was still possible. **B**) Specific activity of *Ps*NosZ (V) with N_2O as a substrate and reduced benzyl viologen as electron donor. The protein was catalytically active, albeit with reduced v_{max} of 1.51 ± 0.06 µM N_2O min^{-1} mg^{-1} and a doubled K_M of 29.78 ± 4.21 µM with respect to *Ps*N_2OR (II) (Figure S3).

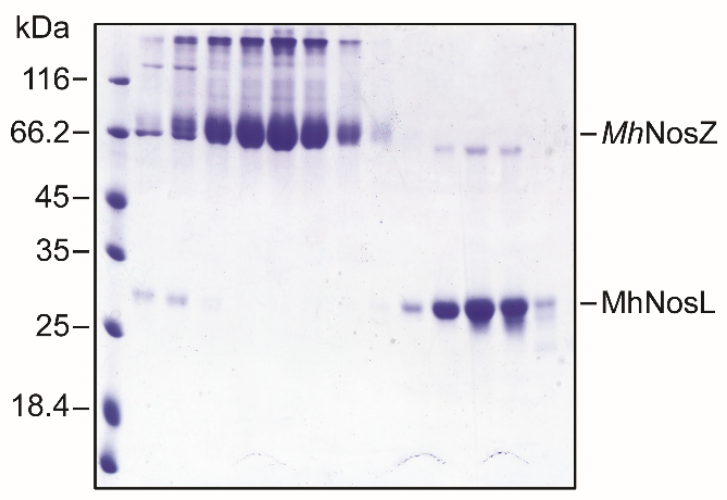

Figure S8: SDS-PAGE analysis of recombinant *Mh*NosZ and *Mh*NosL. Both *Mh*NosZ and *Mh*NosL were Strep-tagged at the C-terminus and separated by size-exclusion chromatography (Superdex 200, GE Healthcare after affinity chromatography). The molecular masses of *Mh*NosZ and *Mh*NosL are 70.3 kDa and 22.7 kDa, respectively. Although Cu_A maturation did not occur, both proteins were produced in soluble form at good yields.

Table S1: Bacterial strains used in this study.

Strains	Genotypes	Sources
E.coli		
XL1-Blue	endA1 gyrA96(nalR) thi-1 recA1 relA1 lac glnV44 F' [::Tn10 proAB+ lacIq Δ(lacZ)M15] hsdR17(rK- mK+)	Stratagene
XL10-Gold	endA1 glnV44 recA1 thi-1 gyrA96 relA1 lac Hte Δ(mcrA)183 Δ(mcrCB-hsdSMR-mrr)173 tetR F' [proAB lacIqZΔM15 Tn10(TetR Amy CmR)]	Stratagene
C43(DE3)	F– ompT gal dcm hsdSB(rB- mB-)(DE3)	Lucigen
Denitrifying bacteria		
MK418 (pPR6hE)	*Pseudomonas stutzeri* ZoBell mutant MK418 harboring plasmid pPR6hE.	(1)
DSM-8798	*Marinobacter hydrocarbonoclasticus* strain	DSMZ

Table S2: Plasmids used in this study.

Plasmid	Relevant characteristics	Sources
pET-22b(+)	Expression vector, T7 promoter, Amp^R.	Novagen
pET-30a(+)	Expression vector, T7 promoter, Kan^R.	Novagen
pPR6hE	pUCP22 based plasmid containing *nosRZDFYLtatE* gene cluster of *P. stutzeri* ZoBell, Amp^R.	(1)
pPR6hE-Zs	Insertion of StrepTag into C-terminus of *nosZ.*	This work
pET30-nos(P)	*nosRZDFYLtatE* gene cluster of *P. stutzeri* in pET30a(+).	This work
pET22-nosZL(P)	*nosZLtatE* genes of *P. stutzeri* in pET22b(+).	This work
pET22-nosZ(P)	*nosZtatE* genes of *P. stutzeri* in pET22b(+).	This work
pET30-nosDFYL(P)	*nosDFYLtatE* gene cluster of *P. stutzeri* in pET30a(+)	This work
pLZPs2	*nosDFYtatE* genes of *P. stutzeri* in pET30a(+).	This work
pET30-nosDF*Y(P)	*nosDFYtatE* genes of *P. stutzeri* in pET30a(+), NosF with mutation of E154Q.	This work
pET22b-apbE(P)	*apbE* of *Pseudomonas stutzeri* ZoBell in pET-22b(+)	(2)
pET22b-apbE(P)attP	pET22b-apbE(P) with *attP* (ϕBT1) site.	This work
pET30-nosRZL(P)	*nosRZLtatE* genes of *P. stutzeri* in pET30a(+)	
pET30-nosRZL(P)attB	pET30-nosRZL(P) with *attB* (ϕBT1) site.	This work
pLZPs1	*nosRZLtatE* and *apbE* genes of *P. stutzeri* in pET22b(+)	This work
pET21a-nosZ(syn)	Codon optimized *nosZ* genes of *Shewanella denitrificans* in pET21a(+), Strep-Tagged.	(3)
pET21a-nosR(syn)	Codon optimized *nosR* genes of *S. denitrificans* in pET21a(+), order from LifeTechnologies.	This work
pET30S-nosR(syn)	Codon optimized *nosR* genes of *S. denitrificans* in modified pET30(+), Strep-Tagged.	This work
pET21a-nosL(syn)	Codon optimized *nosL* genes of *S. denitrificans* in pET21a, order from LifeTechnologies.	This work
pET22b-nosL(syn)	Codon optimized *nosL* genes of *S. denitrificans* in pET22b(+),C-terminal 6×His-Tagged.	This work
pET30S-nosL(syn)	Codon optimized *nosL* genes of *S. denitrificans* in pET30a(+), Strep-Tagged.	This work
pET22-nosZ(M)	*nosZ* gene of *Marinobacter hydrocarbonoclasticus* in pET22b(+), C-terminal 6×His-Tagged.	This work
pET22S-nosZ(M)	*nosZ* gene of *M. hydrocarbonoclasticus* in pET22b(+), Strep-Tagged.	This work
pET22-nosL(M)	*nosL* gene of *M. hydrocarbonoclasticus* in pET22b(+), 6×His -Tagged.	This work
pET30S-nosL(M)	*nosL* gene of *M. hydrocarbonoclasticus* in pET30a(+), Strep-Tagged.	This work

Table S3: Primers used in this study.

Primer	Sequence	Description
ZL141	5'-tggagccacccgcagttcgaaaaataagctgttcgagccatc-3'	StrepTag for NosZ
ZL142	5'-tttttcgaactgcgggtggctccaggccggctcgaccatcatg-3'	
ZL143	5'-tatatctccttcttaaag-3'	backbone of pET
ZL144	5'-tgagatccggctgctaac-3'	
ZL145	5'-ctttaagaaggagatatacatatggcttcccgtgaaatc-3'	pET30-nos(P)
ZL146	5'-gttagcagccggatctcagctcctgcttgacgcctc-3'	
ZL155	5'-ctttaagaaggagatatacatatgttcaaagctcaggctac-3'	pET30-nosDFYL(P)
ZL161	5'-ggcagccatatgagcgacaaagattccaag-3'	pET22-nosZL(P)
ZL162	5'-gtggtggctcagcgtcagctcctgcttgacgcctc-3'	
ZL181	5'-tgagcagcagtggtctgaac-3'	pET22-nosZ(P)
ZL182	5'-tcagaccactgctgctcatttttcgaactgcgg-3'	
ZL182b	5'-tcagaccactgctgctcaggtcaagcgccggcg-3'	pET30-nosDFY(P)
CM001	5'-gcttgctgctgctcgatcagccgaccg-3'	NosF(E154Q)
CM002	5'-gagccccacggtcggctgatcgagcag-3'	
ZL153	5'-tgactttcatgaatcgaa-3'	pET30-nosRZL(P)
ZL154	5'-ttcgattcatgaaagtcatttttcgaactgcgggtg-3'	
ZL205	5'-tgacgaaagtgatccagatgatccagcggattggcgaatgggac-3'	pET30-nosRZL(P)*attB*
ZL206	5'-tctggatcactttcgtcaaaaacctggatatagttcctcctttc-3'	
ZL11	5'-ggcagccatatgcttggaggcagggtg-3'	pET30S-nosR(syn)
Strep-R	5'-gtagtcgtcgactcatttttcgaactgcgggtggctccagctctggaagtacaagttc tcgaggctggcaacatt-3'	
ZL29a	5'-cgatggccatggatggtggtccggataccgt-3'	pET22-nosL(syn)
T7-ter	5'-tgctagttattgctcagcgg–3'	
ZL197	5'-ggcagccatatgaaaaaaagagatgatc-3'	pET22-nosZ(M)
ZL198	5'-gtggtgctcgagggccttttcgacgagcatc-3'	
ZL199	5'-agccacccgcagttcgaaaaatgagatccggctgctaac-3'	pET22S-nosZ(M)
ZL200b	5'-ttcgaactgcgggtggctccactcgagggccttttcgac-3'	
ZL49	5'-cggcgatggccatggattccggagatgaacccgag-3'	pET22b-nosL(M)
ZL50	5'-gtggtgctcgagatgggccatttcagactc-3'	

Table S4: Data collection and refinement statistics.

Data sets		**Form I**	**Form II**
PDB ID		6RL0	6RKZ
Space group		*P* 2_1	*P* 2_1
Cell constants	a, b, c [Å]	108.89, 73.34, 136.28	68.89, 76.79, 108.82
	α, β, γ [°]	90.00, 95.07, 90.00	90.00, 93.33, 90.00
Wavelength [Å]		1.36999	1.36998
Resolution limits [Å]		48.91 – 1.78 (1.81 – 1.78)	76.79 – 1.60 (1.79 – 1.60)
Completeness (%)		100 (100)	92.2 (71.6)
Unique reflections		205189	97861
Multiplicity (%)		13.0 (12.0)	7.0 (7.2)
R_{merge}*		0.120 (2.076)	0.076 (1.075)
$R_{p.i.m.}$		0.034 (0.619)	0.031 (0.428)
Mean I/σ (I)		15.7 (1.4)	14.0 (1.5)
$CC_{1/2}$		0.999 (0.492)	0.998 (0.641)
Refinement statistics			
R_{work} / R_{free}		0.17 / 0.20	0.15 / 0.19
No. atoms		19542	10272
Protein		18402	9245
Ligand/ion		136	106
Water		1004	921
B-factor [Å^2]			
Protein		28.54	31.75
Ligand/ion		30.10	43.66
Water		29.73	40.99
R.m.s. deviations			
bond lengths [Å]		0.0180	0.0102
bond angles [°]		1.8115	1.097

Supplementary references

1. Wunsch P & Zumft WG (2005) Functional domains of NosR, a novel transmembrane iron-sulfur flavoprotein necessary for nitrous oxide respiration. *J Bacteriol* 187(6):1992-2001.

2. Zhang L, Trncik C, Andrade SL, & Einsle O (2017) The flavinyl transferase ApbE of Pseudomonas stutzeri matures the NosR protein required for nitrous oxide reduction. *Biochim Biophys Acta* 1858(2):95-102.

3. Schneider LK & Einsle O (2016) The role of calcium in secondary structure stabilization during maturation of nitrous oxide reductase. *Biochemistry*.